Prediction of Parametric Roll Resonance in Longitudinal Regular Waves Using a Non-linear Method

T.M., Ahmed, *University of Southampton*

D.A Hudson, *University of Southampton*

P. Temarel, *University of Southampton*

E.J. Ballard, *Lloyds Register*

ABSTRACT

In this paper two non-linear, time-domain methods are proposed for the prediction of parametric roll resonance in longitudinal regular waves. Using a two-dimensional approach, periodic changes in the underwater hull geometry due to heave, pitch and wave passage are calculated as a first order function of the local breadth and flare at the still waterline in Method (I), and as a higher order function of the local instantaneous breadth in Method (II). The 1-DoF uncoupled equation of motion in roll -with parametric excitation terms- is then solved in the time-domain in the absence of an external roll excitation. Non-linearities in the roll damping and restoring terms are accounted for. The two methods have been applied to a post-Panamax C11 class containership, travelling in longitudinal regular waves. Obtained results demonstrate that the numerical methods succeeded in producing results similar to those available in the literature. Limitations of the methods used are discussed.

Keywords: *Parametric Roll Resonance, Non-linear, Time-domain.*

1. INTRODUCTION

The phenomenon of parametrically excited roll motion has been known to naval architects for almost half a century now (e.g. Paulling, 1961 and Blocki, 1980). In this phenomenon, transversely symmetrical ships may experience extreme roll motions in longitudinal waves i.e. head or following waves. This is explained by reasoning that in longitudinal waves, ships may experience variations in their transverse stability due to time-varying changes in the underwater hull geometry. In the past the concern with parametric roll was mostly for smaller ships in following seas (e.g. De Kat & Paulling, 1989 and Umeda & Hamamoto, 1995). Now the concern is for the vulnerability of large ships in head seas (Dallinga et al, 1998). The problem returned to prominence recently as a result of significant cargo loss and damage sustained by a C11 post-Panamax container carrier on a voyage from Taiwan to Seattle (France et al, 2003). A detailed investigation followed showing that the ship had experienced large roll motions accompanied by significant pitch and yaw motions, resulting from a periodic change of the transverse stability in head seas. The large change of stability was found to be a direct result of the hull form. A substantial bow flare and stern overhang -typical of large container carriers- caused a dramatic difference in the waterline form and, hence, in the transverse stability of the ship (France et al, 2003).

For parametric roll to occur, however, certain conditions need to be satisfied, in particular (France et al, 2003): 1) the encounter frequency is equal or close to twice the natural frequency of roll. 2) The wavelength is of the same order as the ship length. 3) The wave height exceeds a critical level, or threshold value. 4) The roll damping is below a critical level, or threshold value.

Roll damping plays an important role in the development of parametric roll. If the "loss" of energy per cycle caused by damping is more than the energy "gain" caused by the change in stability, the roll angles will not increase and parametric roll will not develop. On the other hand, if the energy "gain" per cycle is more than the energy "loss" due to damping, the amplitude of parametric roll will start to grow (Shin et al, 2004).

Longitudinal waves i.e. head or following seas, cause the largest change in stability and therefore create maximum parametric excitation. While the physical basis for parametric roll is the same in head and following seas, parametric roll in head seas is more likely to be coupled with, or at least influenced by, heave and pitch motions of the ship, since these motions are typically more pronounced in head-seas (Shin et al, 2004).

Parametric roll should be limited to finite, though sometimes large, amplitudes of roll angle. This is where the role of non-linear terms comes into play since it is known that in the roll equation of motion non-linear terms tend to stabilize parametric roll. The two major non-linear terms in the roll equation of motion are the hydrostatic restoring and damping terms. Although the actions of both terms have similar consequences in limiting parametric roll, the physics of their actions are different. Non-linearity of the GZ curve at large angles of heel leads to a significant change in the effective restoring terms and, therefore, a significant change in the roll resonant period. Change of the roll resonant period may take the system out of the instability zone. The input of additional energy ceases once the roll achieves a certain angle. As a result, an energy balance in motion is established and roll stabilizes at a certain amplitude, provided that capsizing does not occur. On the other hand, non-linear damping has the tendency to increase with roll velocity, thus, sooner or later it will grow above the damping threshold. The system then dissipates more energy than the input energy from parametric excitation, which also leads to stabilization of the roll amplitude (Shin et al, 2004). Non-linearity of the GZ curve is more important in the stabilization of parametric roll than non-linear damping (Bulian et al, 2003).

In this paper, Methods (I) and (II) have been applied to a post-Panamax C11 class containership, traveling in regular waves. Within the scope of the study special attention is focused on the influence of different operational aspects on parametric roll resonance, e.g. different wave heights, wave headings (head or following seas), encounter frequencies, forward speeds, loading conditions (different KG values), etc. Results obtained demonstrate that Method (II) has succeeded in producing results similar to those available in the open literature, whilst Method (I) has a more limited range of application.

2. NUMERICAL SIMULATION

In the literature many of the studies predicting parametric roll resonance are based on the assumption that the ship is a 3-DoF system in heave, pitch and roll. The heave and pitch motions are solved simultaneously and independently of the roll motion, an assumption that is justified experimentally (Oh et al, 2000). However, due to the heave-pitch-roll coupling, heave and pitch motions, together with the wave passage, are an effective amplitude and frequency of excitation in parametric roll. The uncoupled equation of motion in roll is then solved in the absence of an external roll excitation and with non-linearities accounted for in the roll damping and restoring moment (Neves et al, 1999). In other words, the heave and pitch motions feed in the energy required for parametric roll to occur but no reverse influence is exerted by roll on heave and pitch since there is no direct excitation in roll.

In the study presented here and based on the assumptions mentioned previously, two non-linear time-domain methods are adopted and developed. Initially, the heave and pitch equations of motion are solved simultaneously and independently of the roll equation. This solution is obtained using a three-dimensional frequency-domain source distribution method (pulsating source method) which also provides the hydrodynamic data of the ship in roll (added inertia and linear damping). In Method (I), periodic changes in the underwater hull geometry due to heave, pitch and the wave passage are calculated as a first order function of the local breadth and flare at the still waterline, (Neves et al, 1999, and Neves et al, 2003). On the other hand, in Method (II), the periodic changes are calculated as a higher order function of the local instantaneous breadth, i.e. at every time step. In both cases these calculations are carried out using a two-dimensional approach for sections along the length of the ship. The formulation of Method (II) leads to a mathematical model with second order non-linearities defined in terms of the heave-pitch-wave passage couplings. Non-linearities in the roll restoring arm (Surendran et al, 2003) and roll damping (Himeno, 1981) are also accounted for. Finally, the 1-DoF uncoupled equation of motion in roll is solved in the time-domain, subjected to an initial roll angle, using a fourth-order-Runge-Kutta method in the absence of an external roll excitation.

2.1 Mathematical Formulation

For both aforementioned methods, the restoring coefficient in roll may be expressed as:

$$C_{44}(x,t) = \rho g \int_L A(x,t) GM_T(x,t) dx \qquad (1)$$

where, x denotes the coordinate along the ship and A(x,t) represents the immersed sectional area, such that:

$$A(x,t)GM_T(x,t) = I_T(x,t) + Z_b(x,t)A(x,t) - Z_g A(x,t) \qquad (2)$$

where, $I_T(x,t)$ and $Z_b(x,t)$ represent the transverse second moment and the vertical coordinate of the immersed sectional areas, respectively, and $Z_g(x,t)$ represents the vertical coordinate of the ship's centre of gravity.

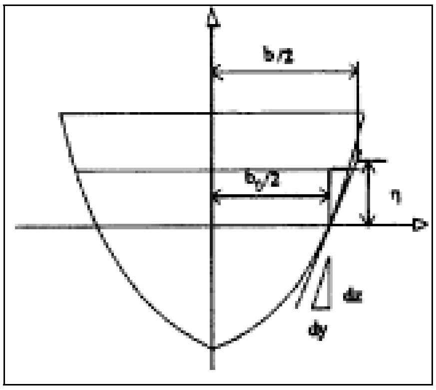

Figure (1) Variation of Sectional Beam with Relative Vertical Displacement

Therefore, for Method (I):

$$C_{44}(x,t) = \Delta g GZ + \rho g \int_L [\frac{1}{2} b_0^2 \left.\frac{dy}{dz}\right|_{x,z=0} - Z_g b_0(x)] \eta dx \qquad (3)$$

and for Method (II):

$$\begin{aligned} C_{44}(x,t) &= \Delta g GZ + \rho g \{ \int_L \alpha(x,t) \\ &[\frac{1}{2} b_0^2(x) + b_0(x)\alpha(x,t) + \frac{2}{3}\alpha^2(x,t)] dx \\ &- Z_g \int_L [b_0(x) + \alpha(x,t)] \eta(x,t) dx \\ &+ \int_L [\frac{1}{2} b_0(x) + \frac{2}{3}\alpha(x,t)] \eta(x,t) |\eta(x,t)| dx \} \end{aligned} \qquad (4)$$

where, as shown in fig.(1) (Neves et al, 1999),

$$\alpha(x,t) = b(x,t) - b_0(x). \qquad (5)$$

The relative vertical displacement η is expressed as:

$$\eta(x,t) = z_0 \cos(\omega_e t + \alpha_z) - x\theta_0 \cos(\omega_e t + \alpha_\theta) - \zeta \cos[kx\cos(\chi) - \omega_e t] \quad (6)$$

where, z_0, θ_0, α_z, α_θ are the heave and pitch magnitudes and phase angles, respectively, ζ is the wave amplitude ω_e is the encounter frequency, k is the wave number and χ is the wave heading.

The normalized 1-DoF uncoupled equation of motion in roll for a ship travelling in longitudinal regular waves takes the form:

$$\ddot{\phi} + (b_{44L} + b_{44N})\dot{\phi} + [c_{44L} + c_{(44N)_3}\phi^2 + c_{(44N)_5}\phi^4 + e_0(t)]\phi = 0 \quad (7)$$

In equation (7), b_{44} and b_{44N} represent the linear and the equivalent linearized roll damping components, respectively. Based on the expression for (ΔgGZ) described in section (2.2), c_{44L}, $c_{(44N)3}$ and $c_{(44N)5}$ represent the linear, cubic polynomial and quintic polynomial roll restoring coefficients, respectively. $e_0(t)$ is the total parametric excitation term (1st and 2nd order) due to heave, pitch and wave passage and can be identified from equations (3) and (4). All coefficients in equation (7) are normalized with respect to the total roll moment of inertia (I_{44}+A_{44}), where I_{44} and A_{44} are the moment and added moment of inertia in roll, respectively.

2.2 Non-linear Roll Restoring Coefficients

As was mentioned before, the non-linear roll restoring coefficients representing the GZ curve have an important role in stabilizing the parametric roll motion of a ship. In the methods presented here, a quintic polynomial expression is used to account for the non-linearity in the GZ curve (Surendran et al, 2003). The righting arm curve is expressed as:

$$\Delta gGZ = C_{44L}\phi + C_{(44N)_3}\phi^3 + C_{(44N)_5}\phi^5 \quad (8)$$

Coefficients of the polynomial are determined by the static and dynamic characteristics of the GZ curve such as the metacentric height, GM_T; the angle of vanishing stability, ϕ_V; and the area under the GZ curve $A_{\phi v}$ up to the angle of vanishing stability as follows (C_{44L}=ΔgGM_T):

$$C_{(44N)_3} = \Delta g[\frac{4}{\phi_v^4}(3A_{\phi_v} - GM_T\phi_v^2)]$$
$$C_{(44N)_5} = -\Delta g[\frac{3}{\phi_v^6}(4A_{\phi_v} - GM_T\phi_v^2)] \quad (9)$$

2.3 Roll Damping

In the methods proposed in this paper, a semi-empirical model due to Ikeda and described by Himeno (1981) is used for the prediction of the total roll damping coefficient. This model assumes that the total roll damping coefficient can be calculated as the sum of five major components, namely: wave damping, frictional damping, eddy damping, lift damping and bilge keel damping.

Out of these five components the wave and lift damping coefficients are assumed linear, whereas the frictional and eddy damping coefficients, together with part of the bilge keel damping coefficient are taken as equivalent linearized damping coefficients, i.e. they are functions of the steady roll angle (through an iteration process for the roll angle and the value of a roll damping) but are proportional to the roll velocity in the roll equation of motion.

3. RESULTS

Methods (I) and (II) have been applied to a post-Panamax C11 class containership (L=262 m), travelling in longitudinal regular waves at two different loading conditions represented by: KG=17.55 m, figs.(2-11) and KG=17.95 m, figs.(12,13). The first loading condition results in a metacentric height GM_T=1.615 m and a roll natural frequency ω_n=0.2673 rad/s. The second loading condition results in a GM_T=1.215 m and ω_n=0.2314 rad/s.

Most of the results have been obtained in two sea-states, namely, sea-state 6, SS(6), and sea-state 7, SS(7), where both are realistic sea-states occurring in the North Atlantic (Faltinsen, 1990). For SS(6) the mean significant wave height is H_w=5 m and the most probable modal wave period is T_w=12.4 s, for SS(7), H_w=7.5 m and T_w=15 s.

Special attention has been paid to the frequency tuning condition of $\omega_e = 2\omega_n$, since this is the first and most dangerous instability zone that arises from solving the damped Mathieu equation for parametric roll.

4. DISCUSSION OF RESULTS

Fig.(2) illustrates the case of the C11 containership advancing in regular head-waves of wave height H_w=8.4 m and wave period T_w=14 s, with a forward speed V=10 knots and an encounter frequency ω_e=0.5544 rad/s. The simulation obtained using Method (I) fails to predict a steady parametric roll angle for this case since the resultant roll angles become very large after approximately t=50 s. This can be attributed to the fact that Method (I) is based on the assumption that the parametric excitation terms are linearized about the still waterline which is justified only for the case of small vertical motions due to small wave heights. On the other hand, Method (II) predicts parametric roll which steadies at a roll angle of 20^o. This agrees with the results predicted for the same case by France et al. (2003) and Shin et al. (2004). On the other hand, fig.(3) represents parametric roll predicted using Methods (I) and (II) for a wave height of 1.5 m and a wave length of 262 m which is equal to the ship length. The ship is travelling in regular head-waves at a forward speed V=4.025 knots. The results predicted by both methods are quite close since at such a small wave height, the higher order terms in Method (II) are insignificant. The difference of 5^o between the steady roll angles predicted by the two methods is due to evaluating the instantaneous local breadth in Method (II) rather than the local breadth and flare at the still waterline in Method (I). In most of the remaining examples, Method (I) fails to simulate parametric roll.

The comparison between fig.(4) and fig.(5) illustrates the importance of the condition, "The wavelength is of the same order as the ship length" in the occurrence of parametric roll. Although SS(6) has a smaller wave height than SS(7), parametric roll is predicted, by Method (II), in fig.(4) but not in fig.(5). This is due to the fact that the wavelength of SS(6), λ=240 m (corresponding to T_w=12.4 s) is closer to the ship length, L=262 m, than that of SS(7), λ=351 m. It should be noted that in fig.(5), the value of the steady roll angle is almost equal to the value of the initial roll angle, hence this is interpreted as a case of non-occurrence of parametric roll.

The comparison between figs.(4), (6) and (7), all for SS(6), demonstrates that the frequency tuning condition of $\omega_e=2\omega_n$ is not always the worst case scenario in parametric roll. While in fig.(4) a steady roll angle of approximately 18^o is predicted at $\omega_e=2\omega_n$, the steady roll angle increases to 28^o and 43^o in figs.(6) and (7) respectively, for different tuning conditions. This can be interpreted by reasoning that the roll natural frequency ω_n is assumed to be constant when it actually varies with time. One should also note that heave and pitch responses will change with changing forward speed.

Figs.(6-8) demonstrate the influence of varying the ship's forward speed on parametric roll, all for SS(6). While in figs.(6) and (7), parametric roll is predicted at forward speeds of V=6 and 12 knots respectively, parametric roll is not predicted in fig.(8) at a forward speed of V=18 knots. This can be attributed to the fact that forward speeds of 6 and 12 knots give encounter frequencies that are close to the encounter frequency of the first instability zone i.e. $\omega_e = 2\omega_n$. On the other hand, changing the forward speed to V=18 knots moves the system out of the instability zone and its vicinity.

In fig.(7), for SS(6), extreme roll motions of 43^o were obtained when using a predicted total roll damping coefficient b_{44} of 0.04. When b_{44} was increased by 33%, to be 10% of the critical roll damping (0.05346), parametric roll is no longer observed. This illustrates the importance of an accurate prediction of the non-potential flow roll damping especially for the “just on the edge” cases of parametric roll.

Fig.(9), for SS(7), shows another comparison between Methods (I) and (II). While Method (I) predicts parametric roll for the investigated case, Method (II) does not. This can be explained by reasoning that Method (I) tends to overestimate the parametric roll predictions as also demonstrated in fig.(3).

Figs.(10) and (11) compare results obtained for the same conditions (zero forward speed, H_w=5 m) in head and following seas using Method (II). They show that the behaviour is similar in both headings. While no parametric roll is seen in the predictions in fig.(10) for a frequency tuning condition of $\omega=\omega_e=\omega_n$, parametric roll of approximately 20^o is detected at a frequency tuning condition of $\omega=\omega_e=2\omega_n$.

The comparison between figs.(5) and (12) demonstrates the influence of reducing the initial GM_T by 0.4 m on parametric roll. While in fig.(5) no parametric roll is predicted in SS(7) and at a frequency tuning condition of $\omega_e=2\omega_n$, parametric roll of up to 15^o is predicted in fig.(12) for the same sea-state and tuning condition. This illustrates the influence of GM_T in the onset of parametric roll.

Finally, in fig.(13), parametric roll of 18^o is again predicted for the lower initial GM_T, this time in following seas (SS(6)) and at a forward speed, V=3.264 knots giving a frequency tuning condition of $\omega_e=2\omega_n$.

5. CONCLUSIONS AND FUTURE WORK

In this paper, two methods have been presented for the prediction of parametric roll resonance in longitudinal regular waves. While Method (I) fails to obtain steady roll angles of parametric roll in the case of large wave heights, the results shown here demonstrate that Method (II) succeeds. Nevertheless, even in such large wave heights, Method (I) does provide an indication of the occurrence of parametric roll.

It is shown (e.g. fig.(2)) that Method (II) reproduces results that are available in the literature and are predicted by other numerical methods. Furthermore, Method (II) is capable of simulating and accurately predicting typical operational scenarios.

From an operational point of view, changing the forward speed of the ship can reduce the likelihood of parametric roll occurring if the change in speed moves the system out of the instability zone.

The frequency tuning condition of $\omega_e=2\omega_n$ is not always the worst case scenario in parametric roll resonance. One has to interpret this tuning condition over a wider range of encounter frequencies. Furthermore, metacentric height GM_T plays an important role, together with operational conditions, in influencing this tuning and, thus, the onset of parametric roll.

Accurate predictions of the total roll damping (linear and non-linear) are essential for any method that predicts parametric roll.

The few results presented in this paper on following seas demonstrate that parametric roll can occur in following seas, as in head seas, if the conditions for occurrence, i.e. wave height, wavelength, encounter frequency tuning are satisfied.

Further developments of this work will include:

- Extending Methods (I) and (II) to arbitrary wave headings.

- Testing the capability of Method (II) to simulate the effects of changes in hull geometry.
- Applying Methods (I) and (II) to various hull forms, sea-states, operational conditions, etc and further verifying results against available published data.
- Extending an available partly non-linear three-dimensional method (hydrostatic and incident wave components) to simulate parametric roll resonance and comparing results with those of Methods (I) and (II).

6. REFERENCES

Blocki, W., 1980, "Ship Safety in Connection with Parametric Resonance of Roll", International Shipbuilding Progress, Vol. 27, no. 306, pp. 36-53.

Bulian, G.., Francescutto, A., and Lugni, C., 2003, "On the Non-linear Modeling of Parametric Rolling in Regular and Irregular Waves", Proceedings of 8th International Conference on the Stability of Ships and Ocean Vehicles (STAB'03), Madrid, Spain, pp. 305-323.

Dallinga, R.P., Blok, J.J., and Luth, H.R., 1998, "Excessive Rolling of Cruise ships in Head and Following Waves", RINA International Conference on Ship Motions and Manoeuvrability, Royal Institution of Naval Architects, London.

De Kat, J.O. and Paulling, J.R., 1989, "The Simulation of Ship Motions and Capsizing in Severe Seas", Transactions of the Society of Naval Architects and Marine Engineers, Vol. 97.

Faltinsen, O.M., 1990, Sea Loads on Ships and Offshore Structures, p.32, Cambridge University Press.

France, W.N., Levadou, M., Treakle, T.W., Paulling, J.R., Michel, R.K. and Moore, C., 2003, "An Investigation of Head-sea Parametric Rolling and its Influence on Container Lashing Systems", Marine Technology, Vol. 40, no. 1, pp. 1-19.

Himeno, Y., 1981, "Prediction of Ship Roll Damping –State of the Art", Dept. of Naval Architecture and Marine Engineering, The University of Michigan, Report no. 239.

Neves, M.A.S., Perez, N. and Valerio, L., 1999, "Stability of Small Fishing Vessels in Longitudinal Waves", Ocean Engineering, Vol. 26, pp. 1389-1419.

Neves, M.A.S., Perez, N. and Lorca, O., 2003, "Analysis of Roll Motion and Stability of a Fishing Vessel in Head-seas", Ocean Engineering, Vol. 30, pp. 921-935.

Oh, I.G.., Nayfeh, A.H. and Mook, D.T., 2000, "A Theoretical and Experimental Investigation of Indirectly Excited Roll Motions in Ships", Philosophical Transactions of the Royal Society, Vol. 358, pp. 1853-1881.

Paulling, J.R., 1961, "The Transverse Stability of a Ship in a Longitudinal Seaway", Journal of Ship Research, Vol. 4, no. 4, pp. 37-49.

Shin, Y.S., Belenky, V.L., Paulling, J.R., Weems, K.M. and Lin, W.M., 2004, "Criteria for Parametric Roll of Large Container Ships in Longitudinal Seas", SNAME Annual Meeting, Washington DC.

Surendran, S. and Venkata Ramana Reddy, J., 2003, "Numerical Simulation of Ship Stability for Dynamic Environment", Ocean Engineering, Vol. 30, pp. 1305-1317.

Umeda, N., and Hamamoto, M., 1995, "Model Experiments of Ship Capsize in Astern Seas", Journal of the Society of Naval Architects of Japan, Vol. 177, pp. 207-21

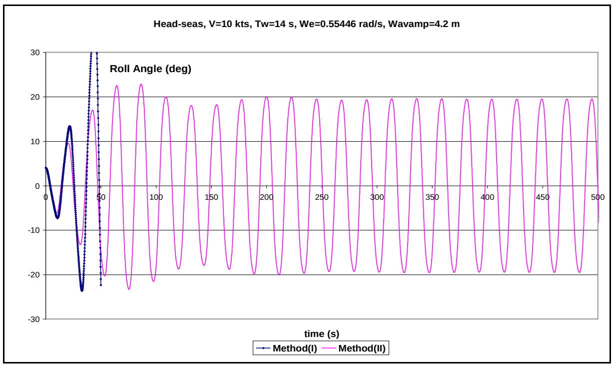

Figure (2) Illustration of parametric roll in regular head waves, predicted b_{44}=0.025

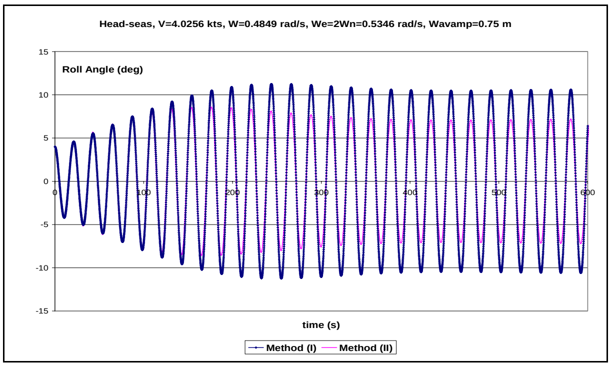

Figure (3) Illustration of parametric roll in regular head waves, predicted b_{44}=0.0125

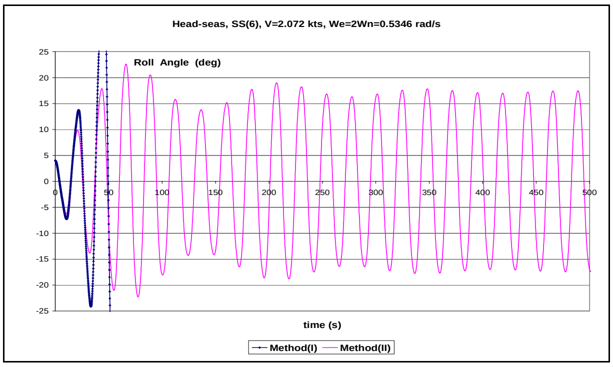

Figure (4) Illustration of parametric roll in regular head waves, predicted b_{44}=0.015

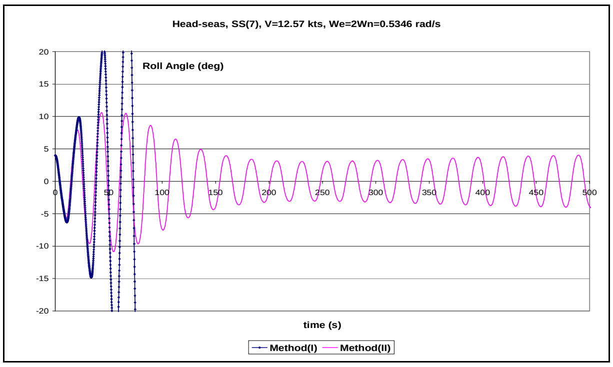

Figure (5) Illustration of parametric roll in regular head waves, predicted b_{44}=0.02

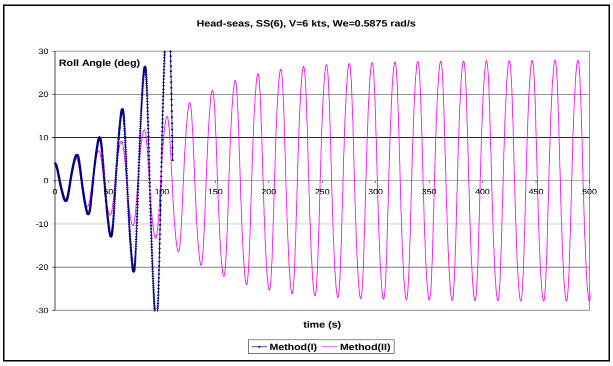

Figure (6) Illustration of parametric roll in regular head waves, predicted b_{44}=0.06

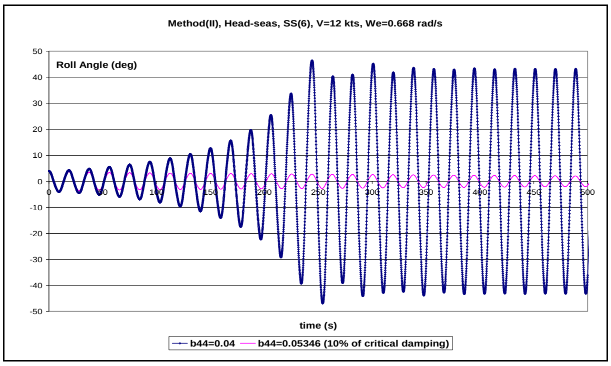

Figure (7) Illustration of parametric roll in regular head waves

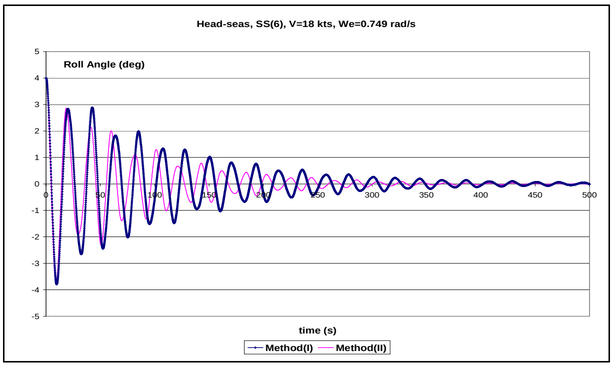

Figure (8) Illustration of parametric roll in regular head waves

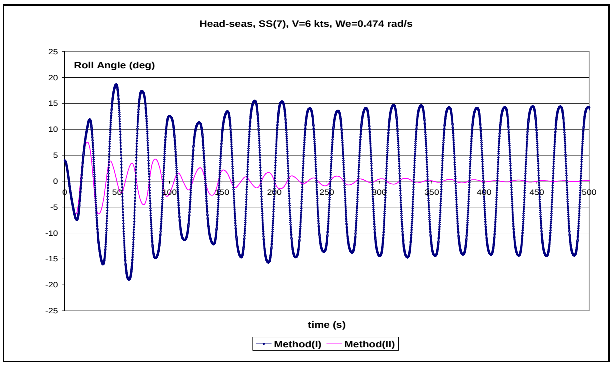

Figure (9) Illustration of parametric roll in regular head waves, predicted b_{44}=0.017

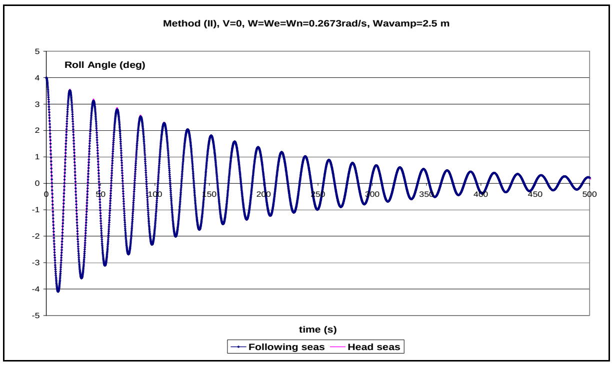

Figure (10) Illustration of parametric roll in regular following and head waves

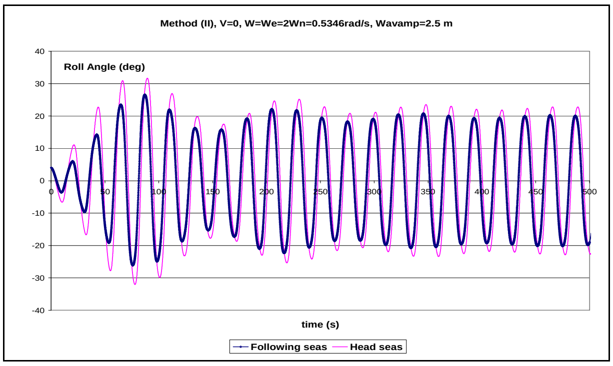

Figure (11) Illustration of parametric roll in regular following and head waves, predicted b_{44}=0.013

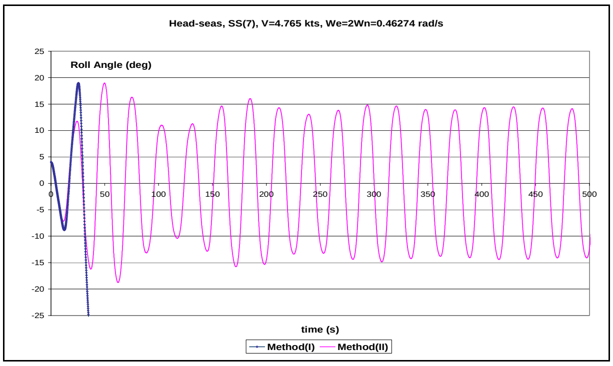

Figure (12) Illustration of parametric roll in regular head waves, KG=17.95 m, predicted b_{44}=0.015

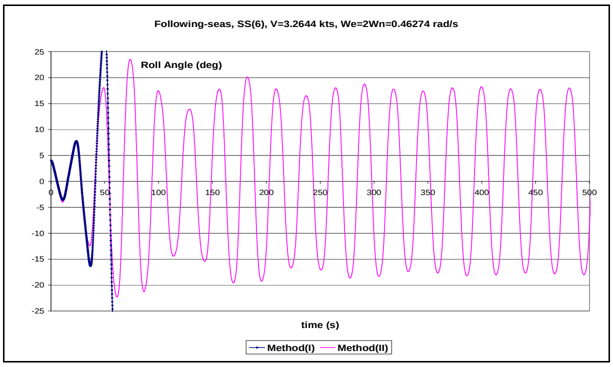

Figure (13) Illustration of parametric roll in regular following waves, KG=17.95 m, predicted b_{44}=0.0156